Dispersive shock water waves. Experiments and numerical comparisons

O. Kimmoun[1*], H.C. Hsu[2], A. Chabchoub[3]

[1] Aix-Marseille University, CNRS, Centrale Marseille, IRPHE, Marseille, France
[2] Tainan Hydraulics Laboratory, National Cheng Kung University, Taiwan
[3] The University of Sydney, Australia

[*] *correspondance : olivier.kimmoun@centrale-marseille.fr*

1 Introduction

Shock waves are non stationnary wave trains characterized by a localized steep gradient across the shock front. This steep gradient is commonly named gradient catastrophe and it is the main mechanism of shock formation [1]. In classical shock wave, dissipation plays a role as regulation mechanism. A different type of shock wave is the dispersive shock waves (DSW) that are also non-stationary wave trains that form spontaneously in weakly dispersive media [2]. It corresponds to a sharp soliton front connected to a rapidly varying oscillatory wave with structure envelope. In this case, dispersion is the regularization mechanism. These DSW are usually observed in shallow water and they are called undular bores [3][4][5]. Laboratory investigations of undular bores was pioneered by Favre as early as 1935[6]. The considered waves correspond to a positive elevation of the free surface. Recently Trillo et al. (2016)[7] performed experiments for a negative elevation and found a very good agreement with the Korteweg–de Vries model.
DSW are also observed in various other media as optics, plasmas, superfluids, gas dynamics or Bose-Enstein Condensate. The experimental observations of such waves was reported first in 1970 for plasma [8]. Recently Fatome et al. (2014)[9] have shown experimentally and numerically for light propagation in optical fibers that wave breaking leads to the observation of multiple optical dispersive shocks and their interaction under different for-wave mixing configurations.
In this paper, we report the results of an experimental campaign performed in a 200m wavetank with a bathymetry that consists with two flat parts connected by a 1/20 slope. When breathers propagates over this bottom, dispersive shock waves are observed that are very similar to those showed by Fatome et al. (2014)[9].

2 Mathematical model

The mathematical model used to generate the modulated wave train is given by the NLSE. This equation describes the space-time evolution of the envelope amplitude $A(x,t)$ of a weakly nonlinear wave train propagating in various media. In arbitrary depth this equation is given by:

$$i\left(\frac{\partial A(x,t)}{\partial t}+c_g\frac{\partial A(x,t)}{\partial x}\right)-\alpha\frac{\partial^2 A(x,t)}{\partial x^2}-\beta|A(x,t)|^2A(x,t)=0 \tag{1}$$

where c_g is the group velocity, α the dispersion coefficient and β the nonlinearity coefficient (see [10] for details). This equation can be rewritten in a non dimensional form given by:

$$\mathrm{i}\,\psi_\xi+\psi_{\tau\tau}+2|\psi|^2\psi=0$$

$$\text{with}\quad \xi=x-C_gt,\quad \tau=-\alpha t\quad\text{and}\quad \psi(\xi,\tau)=\sqrt{\frac{\beta}{2\alpha}}A(\xi,\tau)$$

In the coordinate system (ξ,τ) propagating at the group velocity, a first order solution of this equation is given by Akhmediev [**?**]:

$$\psi(\tau,\xi)=a_0\frac{\sqrt{2\mathfrak{a}}\cos(\Omega\tau)+(1-4\mathfrak{a})\cosh(2R\xi)+\mathrm{i}R\sinh(2R\xi)}{\sqrt{2\mathfrak{a}}\cos(\Omega\tau)-\cosh(2R\xi)}\exp(2\mathrm{i}\xi)$$

$$\text{with} \quad \Omega = 2\sqrt{1-2\mathfrak{a}}, \quad R = \sqrt{8\mathfrak{a}(1-2\mathfrak{a}^2)} \quad \text{and} \quad \mathfrak{a} < 0.5$$

The parameter $\mathfrak{a}$ is the breather parameter. The envelope period is function of this parameter and the initial amplitude of the wave train a_0.

3 Experimental setup

These experiments were conducted at the Tainan Hydraulics Laboratory (THL) of the National ChengKung University in Taiwan in the basin called "Mid-size Observation Flume". The length of the basin is 200m, the width is 2m and the water depth was fixed to h_0=1.3m. One end of the basin is equipped with a piston wavemaker. The bathymetry consists in a constant part of 35m, a 1/20 slope over 20m and again a constant part beyond. With the initial water depth set to 1.3m, the water depth over the second constant part is 0.3m.
To measure the evolution of the free surface, 30 capacitive wave gauges were installed, distributed from 3 to 168.6m. A drawing of the experimental setup with the bathymetry and the wave gauges location is given in figure 1.

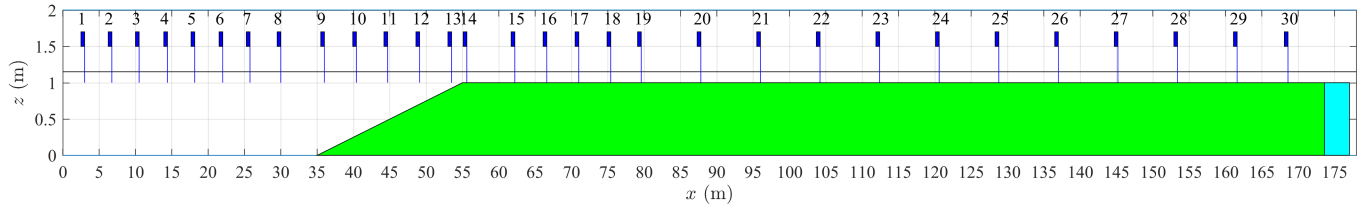

Figure 1: *Drawing of the experimental setup with the bathymetry and the wave gauges location.*

The experimental conditions correspond to different initial k_0h_0 and a_0k_0, with k_0 the wavenumber. Two different breathers are considered, An Akhmediev breather with $\mathfrak{a}$=0.25 and a focusing distance equal to to the edge of the slope at x=55m and a Peregrine breather that corresponds to the limit $\mathfrak{a}$=0.5, with the same focusing distance.

4 Results

4.1 Equation

To compare our results with a numerical code, a NLSE equation in variable bathymetry is considered. This equation was first developed by Djordjevic and Redekoop (1978)[11]. The following equation is the same as for the cited authors but with an adding term to take into account the linear dissipation:

$$\mathrm{i}\left(\frac{\partial A}{\partial x} + \frac{1}{C_g}\frac{\partial A}{\partial t}\right) = -\,\mathrm{i}\,\mu\frac{d(kh)}{dx}A + \lambda\frac{\partial^2 A}{\partial t^2} + \nu|A|^2A + \mathrm{i}\,\frac{\sigma}{C_g}A$$

$$\text{with} \quad \mu = \frac{(1-\sigma^2)(1-kh\,\sigma)}{\sigma + kh(1-\sigma^2)}\,, \quad \lambda = \frac{1}{2C_g\omega_0}\left[1 - \frac{gh}{C_g^2}(1-kh\,\sigma)\left(1-\sigma^2\right)\right]\,,$$

$$\nu = \frac{\omega_0 k^2}{16C_g\,\sigma^2}\left[9 - 10\sigma^2 + 9\sigma^4 - \frac{2C_g^2\,\sigma^2}{gh - C_g^2}\left(4\frac{C_p^2}{C_g^2} + 4\frac{C_p}{C_g}(1-\sigma^2) + 4\frac{gh}{C_g^2}\left(1-\sigma^2\right)^2\right)\right]$$

and σ the dissipation rate. This equation is solved with an usual split-step method.

4.2 A generic example: the Peregrine Breather

In figure 2 the space-time evolution of the envelopes of a Peregrine breather are displayed. The left figure corresponds to the experimental data and the right to the numerical results. Parameters for this case are $\mathfrak{a}$=0.5, T_0=1.2s, h_0=1.3m and a_0k_0=0.11, with T_0 the wave period. The space evolution of the maximum of the normalized envelope is also displayed in figure 3-left. As the wave group reaches the slope, the amplitude of the envelope increases up to the focusing point on the upper edge of the slope and then decreases gradually to the end of the wavetank. The decreases of the envelope is mainly due to the defocusing of the wave group but also due to dissipation that occurs on the frames of the wavetank. This dissipation is known to play in important role on the stability of the wave groups [12][13]. Values of the dissipation rate σ function of the wave period T_0 are computed from previous experiments. When the wave group reaches the upper edge of the slope, waves experience a high gradient that lead to the generation of dispersive shock waves (DSW). This DSW appears as oscillations of the envelope in both sides of the maximum. In figure 3-right the time evolution of the envelopes are displayed for two different distances, one before the slope (10.5m from the wavemaker) and after the edge (128.8m from the wavemaker).

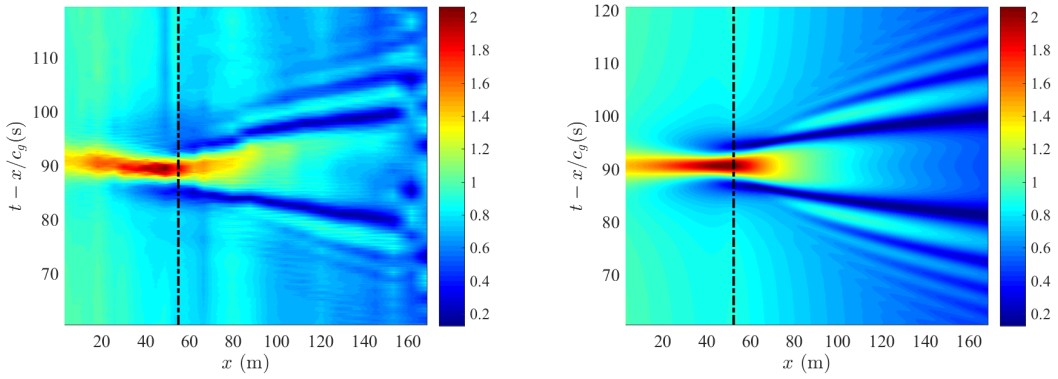

Figure 2: *Space-time evolution of the amplitude of the envelope for a Peregrine Breather case with* $\mathfrak{a}$*=0.5,* T_0*=1.2s,* h_0*=1.3m and* a_0k_0*=0.11. (Left) Experimental, (Right) Numeric.*

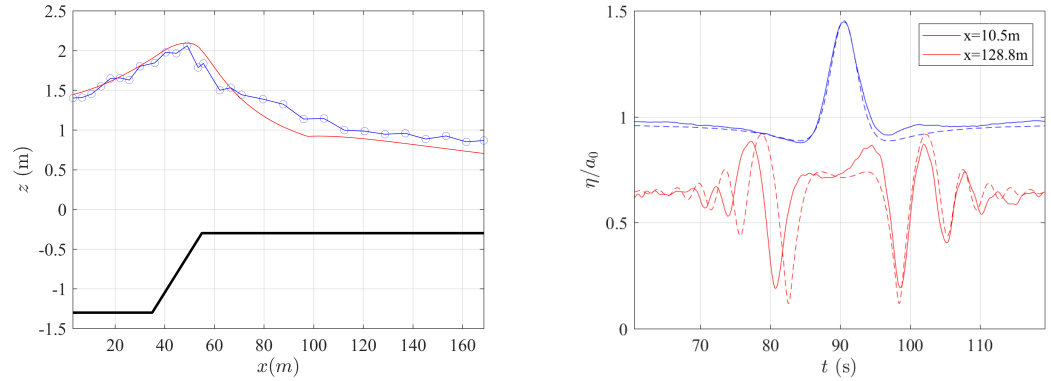

Figure 3: *(Left) Comparison of the maxima of the normalized envelope for the experiments (solid blue line and circles) and for the code (red). The bottom profile is also displayed. (Right) comparison of the time evolution of the envelope for 2 distances from the wavemaker. (Solid lines): experiment, (Dashed lines): numeric.*

On this figure, the oscillation are clearly visible and the comparisons with the numerical model are reasonably good. However some differences are visible. First evolution of the maximum which is symmetric on the model

is asymmetric in the experiments and second the propagation of the shock in the left side of the maxima is not well modelized. These differences might be due to higher dispersion or non linearity effects.

References

[1] G.B. Whitham, Linear and Nonlinear Waves, *Wiley, New York*, (1974).

[2] M. Hoefer & M. Ablowitz, Dispersive shock waves, *Scholarpedia* 4 (11) 5562(2009).

[3] T. B. Benjamin & M. J. Lighthill, On Cnoidal Waves and Bores, *Proc. R. Soc. A* 224, 448 (1954).

[4] D. H. Peregrine, Calculation of the Developments of an Undular Bore, *J. Fluid Mech.* 25, 321 (1966).

[5] R. S. Johnson, Shallow Water Waves on a Viscous Fluid - The Undular Bore, *Phys. Fluids* 15, 1693 (1972).

[6] H. Favre, Etude Théorique et Expérimentale des ondes de Translation dans les Canaux découverts, *Dunod*, (1935).

[7] S. Trillo, M. Klein, G.F. Clauss & M. Onorato, Observation of dispersive shock waves developing from initial depressions in shallow water, *Physica D*, 333, 276-284, (2016).

[8] R. Taylor, D. Baker & H. Ikezi, Observation of collisionless electrostatic shocks, *Phys. Rev. Lett.* 24 (5),206 (1970).

[9] J. Fatome, C. Finot, G. Millot, A. Armaroli, S. Trillo, Observation of Optical Undular Bores in Multiple Four-Wave Mixing, *Physical Review X*, American Physical Society, 4, pp.02102, (2014).

[10] Chabchoub A., Hoffmann N. P. & Akhmediev N. Rogue wave observation in a water wave tank. *Phys. Rev. Lett.*, 106, (2011).

[11] Djordjevic, V. D. & Redekopp, L. G., The fission and disintegration of internal solitary waves moving over two-dimensional topography. *Journal of Physical Oceanography*, 8(6), 1016-1024, (1978).

[12] Kimmoun O., Hsu H.C., Branger H., Li M.S., Chen Y.Y., Kharif C., Onorato M., Kelleher E.J.R., Kibler B., Akhmediev N. & Chabchoub A., Modulation Instability and Phase-Shifted Fermi-Pasta-Ulam Recurrence. *Nature Scientific Reports*, **(6)**28516 (2016).

[13] O. Kimmoun, H.C. Hsu, B. Kibler, & A. Chabchoub , Nonconservative higher-order hydrodynamic modulation instability. *Phys. Rev. E.*, 96(2), 022219, (2017).